J|A|C|S COMMUNICATIONS

Published on Web 07/27/2010

Main-Group and Transition-Element IRMOF Homologues

Steffen Hausdorf, Felix Baitalow, Tony Böhle, David Rafaja,† and Florian O. R. L. Mertens*

Institut für Physikalische Chemie, TU Bergakademie Freiberg, Leipziger Strasse 29, D-09596 Freiberg, Germany

Received April 6, 2010; E-mail: florian.mertens@chemie.tu-freiberg.de

Abstract: A simple two-component procedure was developed to synthesize not only classical zinc-based IRMOFs represented by MOF-5 but also the cobalt and beryllium homologues of this most prominent MOF. The procedure is the first manifestation of mirroring the IRMOF series with other metal centers taken from main-group as well as transition-metal elements. Because of the existence of many suitable precursors, the procedure promises the generation of a large number of IRMOF homologues. Since the IRMOF series together with the MIL series is the MOF group with the largest number of representatives, the possibility of choosing the metal centers of the secondary building units from an extended set will tremendously expand the number of obtainable structures in a predictive, crystal-engineering-type way. Use of metal centers other than zinc will allow the addition of new features to the existing IRMOF structures, such as magnetic properties in the example of cobalt.

The tremendous interest in microporous inorganic−organic hybrid materials was primarily caused by Omar Yaghi's discovery of MOF-5 in 1999.[1] The crystal structure of MOF-5 is composed of tetrahedral $[Zn_4O]^{6+}$ nodes linked by terephthalate ions (BDC^{2-}). The replacement of BDC^{2-} by other linear dicarboxylates led to the IRMOF series, the largest and best-investigated MOF series to date.[2] In IRMOFs, the $M_4O(CO_2)_6$ unit is called the secondary building unit (SBU). It comes as a surprise that even after a decade of research in this area, not a single homologue using a metal other than the original zinc has been published, although significant interest in such materials exists, as expressed by theoretical investigations of electric, magnetic, adsorptive, and diffusional properties.[3] For example, exchanging zinc with light main-group metals such as beryllium and magnesium could lead to an increased gravimetric gas storage capacity, and exchange with transition metals could produce specific catalytic and magnetic properties.

To date, the classical "solvothermal" synthesis protocols based on the exchange of the component zinc nitrate by the nitrates of non-zinc metals have resulted in different structures than IRMOFs only.[4] In this respect it is noteworthy that, as was recently demonstrated, slow oxide formation via nitrate/hydrate decomposition at the zinc centers at low temperatures and pH values is a prerequisite for the formation of IRMOF single crystals.[5] For light metals, it is well-known that such an oxide-forming process does not exist. For divalent heavy metals other than Zn, it must be assumed that this process will not occur under similar conditions, as intermediate $Zn(OH)_x(NO_3)_y$ species display an exceptionally high tendency toward oxide formation through thermal decomposition.[6] Astonishingly, alternative strategies based on the "control SBU approach" (CSA) developed by Férey's group[7] have not been reported either. For IRMOFs, the CSA method would need to be based on the use of precursors consisting of $[M_4O]^{6+}$ nodes with monotopic ligands and the linkage of these nodes to a network by exchanging the monotopic ligands by node-connecting ones. The number of suitable precursors for non-zinc IRMOF homologues is large. Examples for main-group metal precursors containing Be,[8] Mg,[9] or Ca[10] can be found. As an example, Figure 1 shows the molecular structure of tetraberyllium oxohexaacetate, often named "basic beryllium acetate", which is a classical representative of a compound containing tetrahedral μ_4-oxide-bridged metal ions similar to the center of an IRMOF SBU. Analogue complexes based on transition metals such as Zn,[11] Mn,[12,13] Fe,[12] Co,[12,14] Cu,[15] and Au[16] are also known.

To demonstrate the applicability of the method to IRMOFs, we first present the efficient production of conventional, zinc-based MOF-5. As an example of an IRMOF homologue based on a main-group element, we subsequently present the analogously produced and thermally very stable (up to 500 °C) compound MOF-5(Be). The full capability of the CSA method for IRMOF derivatives is demonstrated by the synthesis of the compound MOF-5(Co), which is extremely hydrolysis-sensitive.

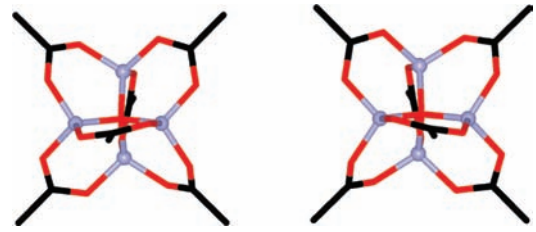

Figure 1. The two enantiomers of $Be_4O(CH_3COO)_6$ (red, oxygen; black, carbon; gray, beryllium). The chirality is caused by the torsion of the carboxylate−Be−O−Be−carboxylate rings.[8b]

MOF-5(Zn). The determination of the ideal reaction conditions advanced through a phase in which the porosity of the obtained MOF material was optimized. The specific pore volume obtained by the *t*-plot method[17] described below was used as the porosity parameter for comparisons.

For the preparation of MOF-5(Zn) by CSA, we used three different procedures: (1) quickly pouring a 0.03 M solution of H_2BDC in either *N*,*N*-dimethyl- or *N*,*N*-diethylformamide (DMF or DEF, respectively) into a solution of the precursor in the same solvent (0.01 M) under rapid stirring; (2) stirring a boiling solution of precursor in acetone with suspended terephthalic acid; and (3) adding a H_2BDC/DEF or H_2BDC/DMF solution (0.03 M) to a stirred solution of the precursor (0.01 M) in the corresponding solvent at a rate of 1.5 mL/min. In all of these syntheses, precursor and linker were used in stoichiometric amounts according to the product $Zn_4O(BDC)_3$. In all cases, the products precipitated from the primary colloidal solutions as microscale particles (<5 μm) within a few minutes. After desolvatization by extraction with

† Present address: Institut für Werkstoffwissenschaft, Gustav-Zeuner-Str.5, D-09596 Freiberg, Germany.

10.1021/ja1028777

CH_2Cl_2 for 8 h and subsequent vacuum drying (0.2−0.5 mbar, 200 °C, 4 h), all of the products were identified as MOF-5 by powder X-ray diffraction (PXRD) and displayed pore volumes in the range 0.11−1.30 cm^3/g. These significant differences may be explained either by the amount of inclusions (e.g., of simple zinc terephthalate) or by partial lattice interpenetration. In addition to variation of the solvent (DEF, DMF, acetone), the optimization procedure included the variation of the method (1−3), the temperature (ambient to 100 °C), and the precursor ligand (acetate, benzoate). As a result of the optimization procedure, it was found that the quality of MOF-5(Zn) produced by CSA improved when the synthesis was carried out at ∼100 °C, using acetate instead of benzoate and DEF instead of DMF, and most importantly, by applying method **3**. CSA MOF-5(Zn) with the highest porosity of 1.30 cm^3/g was produced by adding a solution of terephthalic acid (498 mg, 3 mmol) in DEF (100 mL) to a stirred solution of $Zn_4O(CH_3COO)_6$ (632 mg, 1 mmol) in DEF (100 mL) dropwise over the course of 1 h at 100 °C. The yield after desolvatization was found to be 670 mg (87%).

The pore volume of 1.30 cm^3/g, which was determined from the adsorption curve shown in Figure 2, is comparable to that of solvothermally produced material (1.39 cm^3/g; Saha et al.[18]) and close to the theoretical value of 1.282 cm^3/g calculated from the crystal structure. The Brunauer−Emmett−Teller (BET) surface area of this most porous charge of CSA MOF-5(Zn), as calculated from the low-pressure range of the isotherm, was found to be 3235 m^2/g, which corresponds to 89% of the accessible surface area of perfect crystals given in ref 21a (see the inset of Figure 2 for the BET plot).

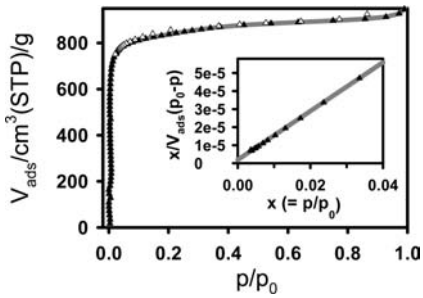

Figure 2. Nitrogen adsorption (▲) and desorption (△) isotherms for MOF-5 synthesized using CSA method **3** at 100 °C. Inset: low-pressure-range BET plot, leading to a monolayer adsorption value of 740 cm^3(STP)/g.

For further information about the reaction conditions, powder patterns, adsorption curves, and other analytical data, see paragraph S4 in the Supporting Information (SI).

MOF-5(Be). Since a basic acetate proved to be a successful medium for the synthesis of highly porous MOF-5(Zn), basic beryllium acetate was chosen as the MOF-5(Be) precursor. Conditions similar to those for the most successful MOF-5(Zn) experiments (method **3**, 100 °C, DEF) provided only amorphous materials with low pore volumes of ∼0.3 cm^3/g. However, crystalline samples could also be obtained by raising the temperature to the boiling points of the solvents (DEF, 179 °C; DMF, 153 °C). The synthesis in DEF using 406 mg (1 mmol) of $Be_4O(CH_3COO)_6$ and all other amounts equal to those for the MOF-5(Zn) synthesis described above yielded 441 mg (81% yield) of the product after desolvatization. The corresponding PXRD pattern was characterized by few highly broadened reflections dominated by a strong reflection at $2\theta = 7.4°$, $d = 12.0$ Å. The existing reflections could be indexed according to the MOF-5 space group, $Fm\bar{3}m$, with a lattice constant of 23.73 Å.

In order to construct a structural model, the assumption was made that the deviation of the lattice constant from that of MOF-5(Zn) (25.76 Å) is exclusively caused by the reduced size of the SBU and not by changes within the linker molecules. Because of the special Wyckoff positions of most of the network atoms, the structural model could be obtained simply by manual calculation. The model was taken as starting configuration for a subsequent Rietveld refinement carried out with the FullProf[19b] software package. A first refinement with fixed atomic positions resulted in a very low Bragg R factor (R_B) of 1.59% but a high overall temperature factor $B = 8\pi^2\langle u^2\rangle = 50.6$ Å^2. Presumably, this high value is caused by a high static Debye−Waller factor. On the basis of the fact that all known basic beryllium carboxylates (see Figure 1) display torsion of the plane spanned by the carboxylate groups relative to the plane spanned by the two adjacent beryllium atoms and the central oxide ion of the SBU,[8b,c] we performed another refinement with an alternative structure model allowing a stochastic occurrence of the torsions in one or the other direction. Because of the nearly ideal planarity of the terephthalate ion in all known structures, one needs to assume that the terephthalate molecule follows the torsion and moves all nonaxis atoms in terephtalate away from the original plane, which corresponds to a mirror plane of the MOF-5 structure. Thus, these atoms change their Wyckoff positions from 96 *k* to 192 *l*. Assuming an equal and random occurrence of the two torsional orientations, the occupancy of these

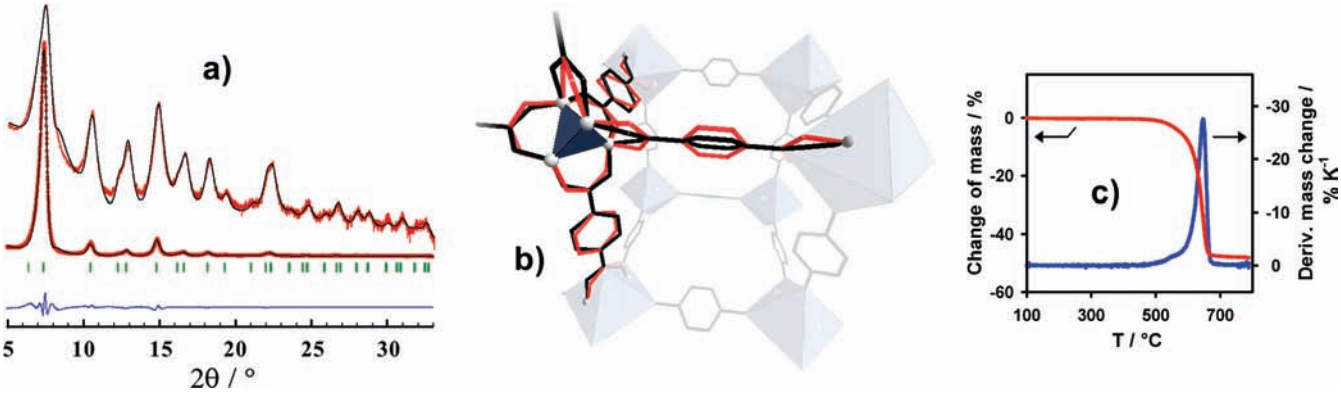

Figure 3. (a) Rietveld analysis of PXRD data for MOF-5(Be). The intensities [logarithmic scale (top curve set) and linear scale (next set below)] of the observed data (red lines) and the refined data (black lines), the difference between them (blue line, linear scale), and the positions of the diffraction lines (green tick marks) are plotted. (b) Structure model of MOF-5(Be). A Be_4O tetrahedron is emphasized, with the Be atoms depicted as white spheres. The terephthalate linkers are drawn in alternative positions in red and black. Schematic extension: $Be_4O(CO_2)_6$ SBUs displayed as octahedrons, with hydrogens omitted for clarity. (c) Thermogravimetric measurement (red) of the decomposition of MOF-5(Be) (Ar stream, 0.2 K/min) and its derivative (blue).

atomic positions must be set to 0.5. As expected, the alternative structure model (also with fixed atomic positions) led to a lower overall temperature factor of 36.0 Å^2 at a still very satisfying R_B of 2.66%. The observed and simulated PXRD patterns are presented in Figure 3a. It is noteworthy that in contrast to MOF-5(Zn), the reflection intensities are dominated by the X-ray scattering of nonmetal atoms. Figure 3b visualizes the atomic distortions occurring in basic carboxylates, on which the alternative model is based.

Additional facts support our claim of having synthesized a MOF-5(Be) homologue:

- The absence of $\nu(CH_3)$ bands in the IR spectra (Figure S4) indicates the full exchange of the acetate. In addition, the lack of all ν(OH) vibrations verifies the absence of hydroxo- or hydrogen terephthalate species.
- The elemental analysis (6.63% Be, 53.58% C, 2.30% H) coincides with the theoretical composition of $Be_4C_{24}O_{13}H_{12}$ (6.62% Be, 52.95% C, 2.22% H).
- The adsorption measurements (see Figure 6; for the *t*-plot, see Figure S6) display a type-1 isotherm and the presence of microporosity. The determined specific pore volume of 1.23 cm^3/g corresponds to 88% of the theoretical value for MOF-5(Be).

The BET surface area was found to be 3289 m^2/g (for the BET plot, see the inset of Figure 6). MOF-5(Be) also proved to be stable up to a temperature of ~500 °C, which is 150 °C higher than MOF-5(Zn) (for the thermogravimetric measurement, see Figure 3c). In contrast to MOF-5(Zn), MOF-5(Be) did not show any signs of change in the PXRD pattern after 3 weeks of exposure to air and also proved to be stable against an azeotropic ethanol−water mixture (10.5 mol % H_2O; Figure S3).

MOF-5(Co). Co^{II} compounds with individual Co_4O^{6+} nodes are known only in conjunction with sterically demanding, complex ligands.[14a] For availability reasons, we decided to use cobalt oxopivalate, a dimeric compound containing two Co_4O^{6+} units (see Figure 4), as the precursor in order to provide preformed Co_4O^{6+} clusters, expecting that the exchange of the pivalate with terephthalate during CSA would result in the incorporation of monomeric Co_4O^{6+} SBUs into the MOF-5(Co) lattice.

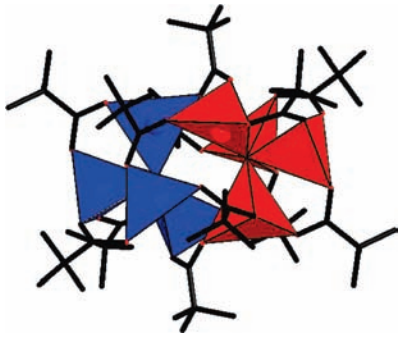

Figure 4. Molecular structure of $Co_8(\mu_4\text{-}O)_2(\mu_n\text{-}OOCCMe_3)_{12}$ according to ref.[14b] The two sets of oxide bridged CoO_4 tetrahedrons contained in the precursor that are each isostructural to the center of the MOF-5(Co) SBU are plotted in red and blue, respectively.

With the use of method **3** with a precursor/DEF solution (858 mg, 0.55 mmol in 100 mL) at 100 °C and a terephthalic acid/DEF solution (498 mg, 3 mmol in 100 mL), a deep-blue precipitate was formed instantaneously. This precipitate (625 mg, 84% yield after desolvatization) was determined to be the cobalt MOF-5 homologue via PXRD and elemental analysis (found: 32.12% Co, 38.47% C, 1.69% H; calcd for $Co_4C_{24}O_{13}H_{12}$: 31.68% Co, 38.74% C, 1.63% H). The complete exchange of pivalate ions was evident by the lack of CH_3 bands in the IR spectrum (Figure S5). The corresponding Rietveld analysis (Figure 5) using as a structure model the original MOF-5 adjusted to a cobalt-containing SBU resulted in an R_B of 6.72%. As expected from the analogy to MOF-5(Zn), the low temperature factor of 2.9 Å^2 does not indicate any torsion of the terephthalate moiety as in MOF-5(Be). MOF-5(Co) proved to be extremely sensitive to hydrolysis, as manifested by a color change from blue to pink upon contact with air moisture. A pore volume of 1.22 cm^3/g was calculated from the measured 77 K nitrogen adsorption isotherm (Figure 6), which corresponds to ~90% of the theoretical value. Low-pressure BET analysis (see the inset of Figure 6) gave a surface area of 3117 m^2/g.

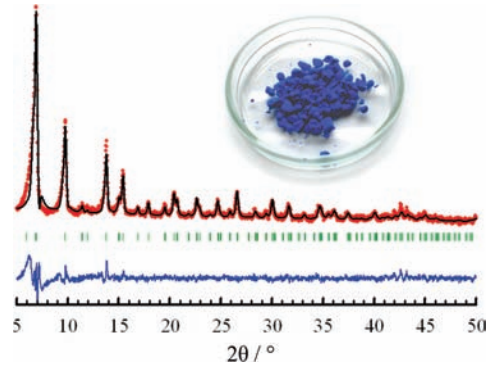

Figure 5. Rietveld analysis of PXRD data for MOF-5(Co). Inset: picture of the synthesized MOF-5(Co). Intensities are plotted on a linear scale.

Porosity Characterization. The pore volume values given in the previous paragraphs were determined using the *t*-plot method, which is based on the capillary condensation phenomenon that occurs in microporous materials. The method distinguishes between the amounts of nitrogen condensed inside the sample particles and on their outer surfaces.[17] The Harkins−Jura equation[20] is used to calculate a thickness parameter t for the outer nitrogen multilayer from the corresponding p/p_0 values. Plotting the total nitrogen uptake versus t and extrapolating to $t = 0$ affords the amount of nitrogen that underwent capillary condensation and thus the specific pore volume (for details, see ref 17 or paragraph S1 in the SI). The specific pore volumes measured were in good agreement with the void volumes calculated from the crystal structures using the PLATON[19a] software. The differences between the corresponding measured and theoretical values of the MOF-5 homologues synthesized via CSA were +1.4% for MOF-5(Zn), −12% for MOF-5(Be), and −10% for MOF-5(Co). The respective *t*-plots can be found in Figures S2, S6, and S7.

Compared with the pore volume, the BET surface area is the more common parameter and can be found in nearly every publication about MOFs. Nonwithstanding this fact, adsorption phenomena in microporous materials do not fulfill some of the original assumptions made in the classical BET theory. In particular, when the interaction of the adsorbed molecules with the pore walls leads to capillary condensation, as is generally the case in microporous materials, erroneous results are obtained from the standard BET analyses.

However, R. Q. Snurr and co-workers[21] have recently shown that a meaningful BET analysis is possible even in such cases if a pressure range well below the standard BET p/p_0 range (typically 0.05−0.3) is used. In order to apply the method to all MOF-5 modifications synthesized by CSA, suitable low-pressure ranges first needed to be identified by finding the p/p_0 ranges for which the plots of $V_{ads}(p_0 - p)$ versus p/p_0 displayed a positive slope.

According to the theory, the positive slope of this function serves as a consistency criterion stating that a meaningful BET analysis can be carried out. For all three MOF-5 materials, the p/p_0 range from 0.0035 to 0.04 in the volumetrically measured 77 K nitrogen isotherms was found to satisfy the consistency criterion and was therefore used in the subsequent analyses.

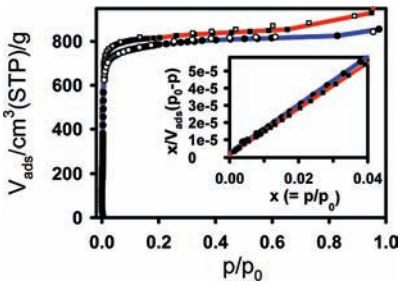

Figure 6. Nitrogen adsorption (solid symbols) and desorption (open symbols) isotherms for the two new MOF-5 homologues, MOF-5(Co) (blue) and MOF-5(Be) (red). Inset: low-pressure-range BET plots, leading to a monolayer adsorption values of 713 cm^3(STP)/g for MOF-5(Co) and 753 cm^3/g for MOF-5(Be).

The corresponding BET plots of $(p/p_0)/[V_{ads}(p_0 - p)]$ versus p/p_0 over the selected p/p_0 range (see the insets of Figures 2 and 5) demonstrate excellent linearity and thus the validity of the analyses for MOF-5(Zn) and the two new MOF-5 homologues based on beryllium and cobalt. The respective specific surface areas of 3235, 3117, and 3289 m^2/g demonstrate that these MOF-5-based compounds synthesized using CSA can be characterized as ultrahigh surface area materials of almost identical porosity, as can also be seen from the almost identical shapes of the isotherms.

Conclusion. Through these experiments, the controlled SBU approach has been demonstrated to be a universal tool for the synthesis of IRMOF structures, opening the door to mirroring of the IRMOF series in many different metal centers. Our results disagree with the general belief that the central oxide ion of the $[M_4O]^{6+}$ unit of a metal(II)−oxo complex would not survive the addition of carboxylic acids in order to conduct the carboxylate exchange.[11b] In this respect, we have demonstrated in previous work that the degree of dissociation of terephthalic acid in DEF is rather low, so protonation of the oxide ion seems unlikely.[5] It is noteworthy that we were not able to synthesize MOF-5(Co) at temperatures above 100 °C because of protonation of the oxide under these conditions. In other experiments not presented here, the synthesis of the aminoterephthalate-based IRMOF-3(Zn) by CSA was successful at 50 °C but not 100 °C. On the other hand, the synthesis of crystalline MOF-5(Be) did not succeed at temperatures lower than 150 °C. As a consequence of such diverse reaction conditions, the term "controlled SBU approach" should be viewed as a specific procedure that encompasses the identification of suitable precursors and the adjustment of the reaction conditions to the precursor and linker used with the purpose of arriving at a specific framework of high porosity. Regardless of the necessary optimization, CSA still comes nearest of all known MOF syntheses to the concept of "crystal engineering". It specifically promises a possible synthesis of MOF-5(Mg) and of sensitive compounds that are otherwise impossible to make.

Acknowledgment. The authors thank the Deutsche Forschungsgemeinschaft for a grant given within the priority program "Porous Metal−Organic Frameworks", SPP 1362. We are grateful to Alexander Münch for experimental support.

Supporting Information Available: Experimental details, crystallographic data for MOF-5(Be) and MOF-5(Co), stability and spectroscopic data, BET and porosity measurements, and evaluation details. This material is available free of charge via the Internet at http://pubs.acs.org.

References

(1) Eddaoudi, M.; Li, H.; O'Keeffe, M.; Yaghi, O. M. *Nature* **1999**, *402*, 276–279.
(2) (a) Eddaoudi, M.; Kim, J.; Rosi, N.; Vodak, D.; Wachter, J.; O'Keeffe, M.; Yaghi, O. M. *Science* **2002**, *295*, 469–472. (b) Rosi, N. L.; Eckert, J.; Eddaoudi, M.; Vodak, D. T.; Kim, J.; O'Keeffe, M.; Yaghi, O. M. *Science* **2003**, *300*, 1127–1129. (c) Duren, T.; Sarkisov, L.; Yaghi, O. M.; Snurr, R. Q. *Langmuir* **2004**, *20*, 2683–2689. (d) Millward, A. R.; Yaghi, O. M. *J. Am. Chem. Soc.* **2005**, *123*, 17998–17999.
(3) (a) Fuentes-Cabrera, M.; Nicholson, D. M.; Sumpter, B. G. *J. Chem. Phys.* **2005**, *123*, 124713. (b) Han, S. S.; Deng, W.-Q.; Goddard, W. A., III. *Angew. Chem., Int. Ed.* **2007**, *46*, 2689–2692. (c) Babarao, R.; Jiang, J. *Langmuir* **2008**, *24*, 6270–6278.
(4) Kim, J.; Chen, B.; Reineke, T. M.; Li, H.; Eddaoudi, M.; Moler, D. B.; O'Keeffe, M.; Yaghi, O. M. *J. Am. Chem. Soc.* **2001**, *123*, 8239–8247.
(5) Hausdorf, S.; Wagler, J.; Mossig, R.; Mertens, F. O. R. L. *J. Phys. Chem. A* **2008**, *112*, 7567–7576.
(6) Biswick, T.; Jones, W.; Pacuła, A.; Serwicka, E.; Podobinski, J. *J. Solid State Chem.* **2007**, *180*, 1171–1179.
(7) Serre, C.; Millange, F.; Surblé, S.; Férey, G. *Angew. Chem., Int. Ed.* **2004**, *43*, 6286–6289.
(8) (a) Urbain, G.; Lacombe, H. *Compt. Rend.* **1901**, *133*, 874–876. (b) Tulinsky, A.; Worthington, C. R. *Acta Crystallogr.* **1959**, *12*, 623–637. (c) Berger, R. J. F.; Schmidt, M. A.; Jusélius, J.; Sundholm, D.; Sirsch, P.; Schmidbaur, H. *Z. Naturforsch.* **2001**, *56b*, 979–989.
(9) (a) Stucky, G.; Rundle, R. E. *J. Am. Chem. Soc.* **1964**, *86*, 4821–4825. (b) Mösch-Zanetti, N. C.; Ferbinteanu, M.; Magull, J. *Eur. J. Inorg. Chem.* **2002**, 950–956.
(10) (a) Ruspic, C.; Harder, S. *Organometallics* **2005**, *24*, 5506–5508. (b) Westerhausen, M. *Z. Anorg. Allg. Chem.* **2009**, *635*, 13–32.
(11) (a) Auger, V.; Robin, J. *Compt. Rend.* **1924**, *178*, 1546–1548. (b) Gordon, R. M.; Silver, H. B. *Can. J. Chem.* **1983**, *61*, 1218–1221. (c) Hiltunen, L.; Leskelä, M.; Mäkelä, M.; Niinistö, L. *Acta Chem. Scand.* **1987**, *A41*, 548–555. (d) Clegg, W.; Harbron, D. R.; Homan, C. D.; Hunt, P. A.; Little, I. R.; Straughan, B. P. *Inorg. Chim. Acta* **1991**, *186*, 51–60.
(12) Cotton, F. A.; Daniels, L. M.; Falvello, L. R.; Matonic, J. H.; Murillo, C. A.; Wang, X.; Zhou, H. *Inorg. Chim. Acta* **1997**, *266*, 91–102.
(13) Yang, C.-I.; Wernsdorfer, W.; Tsai, Y.-J.; Chung, G.; Kuo, T.-S.; Lee, G.-H.; Shieh, M.; Tsai, H.-L. *Inorg. Chem.* **2008**, *47*, 1925–1939.
(14) (a) Jaitner, P.; Veciana, J.; Sporer, C.; Kopacka, H.; Wurst, K.; Ruiz-Molina, D. *Organometallics* **2001**, *20*, 568–571. (b) Siderov, A. A.; Fomina, L. G.; Ponina, M. O.; Aleksandrov, G. G.; Nefedov, S. E.; Eremenko, L. L.; Moiseev, L. L. *Russ. Chem. Bull.* **2000**, *49*, 958–959.
(15) Bock, H.; Dieck, H. T.; Pyttlik, H.; Schnoller, M. *Z. Anorg. Allg. Chem.* **1968**, *357*, 54–61.
(16) Schmidbaur, H.; Hofreiter, S.; Paul, M. *Nature* **1995**, *377*, 503–504.
(17) Lippens, B. C.; de Boer, J. H. *J. Catal.* **1965**, *4*, 319–323.
(18) Saha, D.; Wei, Z.; Deng, S. *Sep. Purif. Technol.* **2009**, *64*, 280–287.
(19) (a) Spek, A. L. *J. Appl. Crystallogr.* **2003**, *36*, 7–13. (b) Roisnel, T.; Rodriguez-Carvajal, J. *Mater. Sci. Forum* **2001**, *378*−*3*, 118–123.
(20) Harkins, W. D.; Jura, G. *J. Chem. Phys.* **1943**, *11*, 431–437.
(21) (a) Walton, K. S.; Snurr, R. Q. *J. Am. Chem. Soc.* **2007**, *129*, 8552–8556. (b) Bae, Y.-S.; Yazaydın, A. Ö.; Snurr, R. Q. *Langmuir* **2010**, *26*, 5475–5483.

JA1028777